Absorption and diffusion of hydrogen in palladium-silver alloys by density functional theory

Xuezhi Ke* and Gert Jan Kramer
Schuit Institute of Catalysis, Eindhoven University of Technology, P.O. Box 513, 5600 MB Eindhoven, The Netherlands
(Received 24 April 2002; revised manuscript received 22 August 2002; published 27 November 2002)

The vibrational states, absorption energies, and diffusions of H in Pd and $Pd_{1-x}Ag_x(0\leqslant x\leqslant 1)$ have been studied by first-principle calculations. All results compare favorably to experiment. The zero-point motion of H is important in the determination of the H site occupation, in the estimation of the diffusion barrier, and in the explanation of the reversed isotope effect. The interesting anomalous isotope effect is explored, and a diffusion mechanism is proposed for tritium. The preferred diffusion paths of H in Pd and $Pd_{1-x}Ag_x$ are ''indirect'' paths. According to the absorption energies and diffusion barriers, H diffusion in Pd-Ag alloys should avoid the Ag-rich areas.

DOI: 10.1103/PhysRevB.66.184304 PACS number(s): 66.30.−h, 31.15.Ar, 31.50.−x

I. INTRODUCTION

The Pd-H system has continuously attracted attention, not only because of its technological application in H storage and separation, but also because of its special place within the more general class of metal hydrides with its an extensive literature.[1–4] Pd is special since it readily dissociates H, stores H at high volumetic density, and has a high H diffusivity. For the different H concentrations at room temperature, there are two phases in PdH_x fcc lattice including the $\alpha(x<0.1)$ phase and the $\beta(x>0.6)$ phase.[5] Both phases exhibit a fcc structure and differ only in their lattice constants. Of particular interest are the alloys of Pd with silver, which are widely employed as a material for the diffusion membranes. Pure Pd is not attractive for practical applications because loading with H induces a structural phase transformation,[1] which causes embrittlement over H loading and unloading cycles. By alloying Pd with Ag, the phase transition and the associated embrittlement can be suppressed.

Over the years, there has been a continued theoretical interest in the vibrational energies, the diffusion, and the dissociation of H in pure Pd,[6–15] but there is little theoretical understanding of H in Pd-Ag alloys. This paper and a recent paper by Løvvik[16] intend to fill this gap. In the present work, the anharmonic excitation energies, absorption energies and activation energies of H in Pd and Pd-Ag alloys are addressed. Our results show that the harmonic approximation is inadequate to study the vibrations of H in the Pd-Ag alloys and the solubility of H in the Pd-Ag alloys increases for a 25% silver concentration. In particular, we stress the influence of the zero-point motion on the absorption and diffusion of H. Besides that, we explore the interesting anomalous isotope effect.[17–20]

The paper is organized as follows. Section II describes the theoretical methods. Section III discusses the main calculation results. Section IV consists of a summary and conclusions.

II. MODEL AND SIMULATION METHODS

For H in pure Pd, the experiment shows that PdH_x $(0\leqslant x\leqslant 1)$ has a face-centered cubic (fcc) crystal structure.[5] H preferentially occupies the octahedral site in the interstitial spaces of Pd fcc lattice.[21–24] To investigate both α and β phase, we performed calculations for several H concentrations in PdH_x ($x=0.03125$, 0.0625, 0.25, 0.5, 0.75, and 1), where x is the ratio of H/Pd. In detail, $PdH_{0.03125}$, $PdH_{0.25}$, $PdH_{0.5}$, and $PdH_{0.75}$ are modeled by the simple cubic cells of $Pd_{32}H$, Pd_4H, Pd_4H_2, and Pd_4H_3, respectively. $PdH_{0.0625}$ is modeled by the tetragonal cell of $Pd_{16}H$. PdH is modeled by one hydrogen and one Pd. The H_2 molecule is modeled by a dimer in a simple cubic supercell. The lattice constant is 10 Å, which is large enough to prevent interaction between two H_2 molecules. The calculated bond length of 0.75 Å for the H_2 molecule agrees well with the experimental value of 0.74 Å.[25]

For the alloy structures, the experiment shows that the majority of binary alloys of Pd with the neighboring elements in the periodical table have fcc compositions.[26] In our study, fcc structures have been assumed for $Pd_{1-x}Ag_x$ ($x=0.0$, 0.25, 0.5, 0.75, and 1.0) alloys, where x is the fraction of Ag. H absorption in $Pd_{1-x}Ag_x$ alloys and in pure silver was modeled by the simple cubic (or tetragonal) cells containing four heavy atoms (Pd or Ag) and one H atom, depicted in Fig. 1. For H in pure Pd, all octahedral sites are crystallographically equivalent. For H in $Pd_{1-x}Ag_x$ alloys, there are two different octahedral sites for H occupations. We specify O_1 and O_2 in each structure, where O_1 is by definition surrounded by more Pd atoms and less Ag atoms. Table I summarizes the specified O_1 and O_2 sites in $Pd_{1-x}Ag_xH_{0.25}$ structures. Figure 1(d) shows a (110) plane of the fcc lattice where the large, filled circles are the positions of Pd (or Ag) atoms. The open circles are octahedral sites. Additionally, the filled squares are the S_{111} transition states and the open squares are the S_{110} transition states for the H diffusion.

The quantum-mechanical study was performed using the Vienna *ab initio* simulation package,[27,28] which allows for periodic density functional theory (DFT) calculations by solving the Kohn-Sham equations (KS) with pseudopotentials and a plane wave basis set. The approach implemented in the program is based on a finite-temperature generalized gradient approximation with the Perdew–Wang 91 functional.[29] The interactions between the ions and the electrons are described by the ultra-soft (US) pseudopotentials introduced by Vanderbilt.[30]

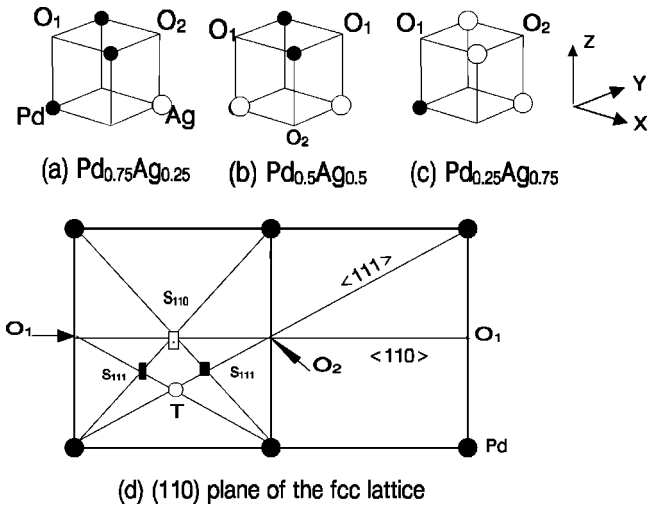

FIG. 1. Cell configurations used in the DFT calculation for Pd-Ag alloys. (a), (b), and (c) are schematic models for the alloys. O_1 and O_2 are octahedral sites. (d) shows a (110) plane of the fcc lattice. Some high-symmetry sites are shown in the plane. The large and filled circles are the positions of Pd or Ag atoms, the small and filled circles are octahedral sites, and the small and open circles are tetrahedral sites. Additionally, the filled squares are the S_{111} transition states and the open squares are the S_{110} transition states.

Brillouin-zone integrations were performed on an $11\times11\times11$ mesh.[31] The energy cutoff is 436 eV. With these basis set, we chose Pd_4H as a test, when the energy cutoff was increased to 500 eV or the mesh was increased to $15\times15\times15$, the changes of total energy in these cases were smaller than 0.5 meV per atom. A Gaussian smearing with 0.2 eV was applied during the geometry optimization. There are two kinds of geometry optimization in our calculation. One just optimizes the coordinates of atoms. This is suitable for a high symmetry cell such as the cubic cell. The other fully optimizes structure including coordinates and lattice vectors (cell volume). This is suitable for a low symmetry cell such as the tetragonal cell. In all calculations, the total energy was converged to be less than 0.5 meV with respect to the **k** point sampling, energy cut-off and cell size. In order to check the accuracy of the US pseudopotentials for our models, the absorption energy (per H atom) of H in the octahedral site of $PdH_{0.25}$ also was calculated by Blöchl's projector augmented wave (PAW) method.[32] There is all-electron description of the electron-ion-core interaction in the PAW. This method is able to describe bulk properties very accurately, the level of accuracy is comparable to FLAPW calculations.[33] The results show that the absorption energy of 0.171 eV calculated by the PAW method is almost the same as that of 0.170 eV by the US pseudopotentials. The energy difference is less than 1%.

Equilibrium lattice constants were obtained by fitting the total energies at different lattice constants to a so-called Rose curve.[34] The calculated lattice constants of $Pd_{1-x}Ag_x$ and PdH_x as a function of x are plotted in Figs. 2(a) and 2(b), respectively. The calculated lattice constants of 3.96 Å for Pd and 4.17 Å for Ag are in good agreement with the experimental values of 3.89 Å and 4.08 Å,[35] respectively. As can be seen in Fig. 2(a), the calculated lattice constants increase almost linearly with increasing Ag concentrations. This behavior is very similar to that of the experiment.[35] Both calculated and measured results in Fig. 2(b) show the lattice constants increase with increasing H concentrations. It is noted that the experimental finding of 0.06-Å lattice difference between pure Pd (Ref. 36) and $PdH_{0.25}$ (Ref. 5) is reproduced in our calculations. The lattice constants for $Pd_{1-x}Ag_xH_{0.25}$ are compiled in Table II.

The vibrational excitations of H in the octahedral sites were calculated using the ANHARMND (Ref. 36) package. The package solves the time-independent Schrödinger equation based on the potential energy surface (PES). The three dimensional (3D) PES is fitted with the polynomial functions in (x,y,z).[37] A fourth-order polynomial was found to fit the PES very well. The deviation of the fit was less than 0.2%. To obtain a reasonable description of the vibrations of H in the octahedral site, a $7\times7\times7$ mesh was chosen, and the step size of H displacement was $0.06\times a_x$ (or a_y or a_z). With this set, the calculated results of PdH and PdD agree well with the experiment. When a more dense mesh is used, the results do not show any clear improvement. The test results are summarized in Table III.

The nudged elastic band method (NEB) (Ref. 38) was used to calculate energy barriers for the H diffusion. Each image in the NEB is only allowed to move into the direction perpendicular to the hyper-tangent, which is calculated as the normal vector between two neighboring images. The algorithm keeps the distance between the images to first order constant. The quasi-Newton algorithm was used to refine the obtained result with the NEB. The forces and the stress tensor are used to determine the search directions to find the equilibrium positions, until they are less than 0.02 eV/Å.

TABLE I. The symbols of O_1 and O_2 are specified for the different octahedral sites of $Pd_{1-x}Ag_xH_{0.25}$. By definition, the octahedral site surrounded by more Pd and less Ag atoms is denoted as O_1, inversely, it is denoted as O_2 in each structure. For H in the pure Pd or pure Ag, O_1 and O_2 sites are identical.

	H in O_1 site surrounded by	H in O_2 site surrounded by
$PdH_{0.25}$	Six Pd atom	Six Pd atoms
$Pd_{0.75}Ag_{0.25}H_{0.25}$	Six Pd atoms	Four Pd and two Ag atoms
$Pd_{0.5}Ag_{0.5}H_{0.25}$	Four Pd and two Ag atoms	Two Pd and four Ag atoms
$Pd_{0.25}Ag_{0.75}H_{0.25}$	Two Pd and four Ag atoms	Six Ag atom
Ag_4H	Six Ag stoms	Six Ag atoms

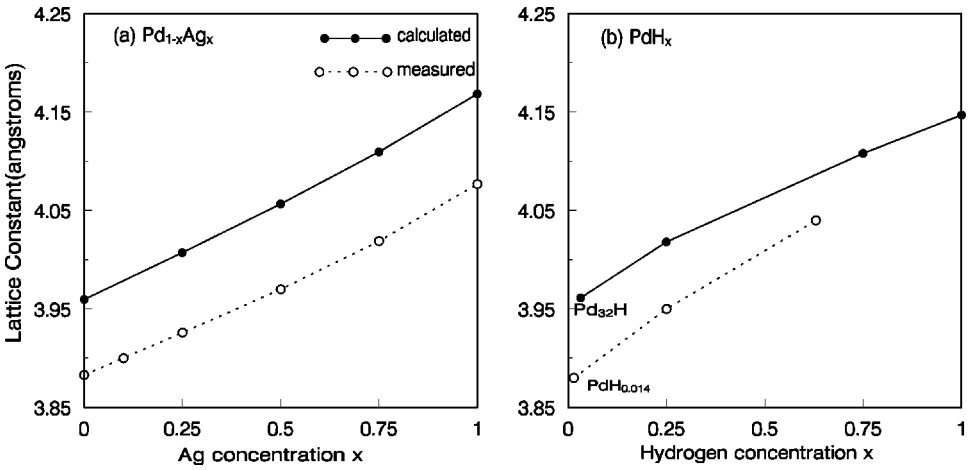

FIG. 2. The calculated (solid circles) and measured (open circles) lattice constants for $Pd_{1-x}Ag_x$ and PdH_x. (a) shows the lattice constants as a function of x in $Pd_{1-x}Ag_x$. The data for $Pd_{0.75}Ag_{0.25}$ and $Pd_{0.25}Ag_{0.75}$ are interpolated from the experiment (Ref. 35). (b) shows the lattice constants of PdH_x as a function of x ($x=0.03125$, 0.25, 0.75, and 1).

III. RESULTS AND DISCUSSIONS

A. Zero-point and excitation energies of the vibrations of H

The zero-point (ZP) and excitation energy of the vibrations of H in the octahedral site of the Pd and Pd-Ag alloys are calculated by solving the time-independent Schrödinger equation.[36] The energy levels are expressed as follows:

$$e_{nml}=E_{nml}-E_{000} \tag{1}$$

where E_{000} is the oscillator ground state energy. n,m and l are the quantum numbers of the harmonic-oscillator states. The calculated energies of H in PdH_x ($x=0.25$ and 1) and $Pd_{1-x}Ag_xH_{0.25}$ ($x=0.25$, 0.5, 0.75, and 1) are compiled in Tables IV and V, respectively.

For H in Pd in our models, H concentrations in PdH_x ($x=0.03125$, 0.0625, and 0.25) and PdH are close to the α phase and the β phase in the experiment,[5] respectively. Figures 3(a) and 3(b) show the ZP and first excitation energies of H in PdH_x as a function of x. Both Figs. 3(a) and 3(b) show that the energies decrease with increasing H concentrations. This can be explained by the fact that the increasing H concentration leads to the increase of the lattice constant, resulting in the shallower vibrational PES, and thus lowing the excitation energy.[39] This was also concluded by Elsässer *et al.*[43] Table IV shows that the calculated results are in good agreement with the experiment[38] and the previous calculations.[6] For H in $PdH_{0.25}$, the energies calculated by Elsässer *et al.* overestimate the energies to some extent. Elsässer *et al.* explained this by lack of the local lattice relaxations during the PES calculations. This does not seem important for the energies if we compare our results with the experiment, indicating that the total-energy calculations are good enough to predict the vibrational energies. To explain inelastic-neutron-scattering spectra,[43] Elsässer *et al.*[6] proposed that two excited states of 137 ± 2 meV and 156 ± 3 meV seem to be the excitations $e^{(1)}_{200}$ and $e^{(2)}_{200}$, respectively. These states are also observed in our calculations. For the higher excitation energies, the mixing among them are clearly observed.

Table V shows the calculated energies of H in $Pd_{1-x}Ag_xH_{0.25}$ alloys. It shows that there are substantial differences between the anharmonic and harmonic potential. This indicates that the harmonic approximation is inadequate for studying the vibrations of H in the alloys. Comparing the corresponding energies of H in $Pd_{0.75}Ag_{0.25}H_{0.25}$ (H in the O_1 site) with those of H in $PdH_{0.25}$ (Table IV), we find the energies in $Pd_{0.75}Ag_{0.25}H_{0.25}$ are slightly smaller than those in $PdH_{0.25}$. This can be explained as before.[39] Moreover, the corresponding energies of H in $AgH_{0.25}$ are slightly smaller than those of H in $Pd_{0.25}Ag_{0.75}H_{0.25}$ for the same reason.[39] For H in some of $Pd_{1-x}Ag_xH_{0.25}$ structures, the energies of e_{001} (z direction) are significantly larger than those of e_{100} (x or y direction). This reflects the fact that the vibrational potential in the z direction is much steeper than that in the x and y directions. There are two reasons for this. One is that Ag atoms make the potential steeper. H in the O_1 site of $Pd_{0.5}Ag_{0.5}H_{0.25}$ and H in the O_2 site of $Pd_{0.75}Ag_{0.25}H$ belong

TABLE II. The calculated lattice constants of $Pd_{1-x}Ag_xH_{0.25}$ ($x=0.25$, 0.5, and 0.75). The lattice vectors along x,y, and z directions are specified as a_x, a_y, and a_z, respectively. Units are in Å.

	H in O_1 site		H in O_2 site	
	$a_x(a_y)$	a_z	$a_x(a_y)$	a_z
$Pd_{0.75}Ag_{0.25}H_{0.25}$	4.063	4.063	3.986	4.227
$Pd_{0.5}Ag_{0.5}H_{0.25}$	4.037	4.260	4.470	3.535
$Pd_{0.25}Ag_{0.75}H_{0.25}$	4.468	3.657	4.173	4.173

TABLE III. The calculated and measured oscillation energies (ω) and the root mean square displacement (rms) of H and deuterium in the octahedral site of bulk Pd (PdH unit cell). rms is calculated from the expression of $\Delta x=\sqrt{\langle x^2\rangle-\langle x^2\rangle}$ (atomic unit). The results are calculated by using two different meshes. Units for the energies are in meV.

	$7\times7\times7$ mesh with the displacement $0.06\times a_x$		Experimental and theoretical results	
	ω	rms	ω	rms
PdH	55.7	0.348	56.0 [a]	0.357 [b]
PdD	37.9	0.300	37.6 [a]	0.305 [c]

[a]Experiment from Refs. 40 and 41.
[b]Theory from Ref. 8.
[c]Experiment from Ref. 42.

TABLE IV. The calculated and measured excitation energies of the vibrations of H in the octahedral sites of PdH and $PdH_{0.25}$ (in meV). α and β samples in experiment (Ref. 43) are $PdH_{0.014}$ and $PdH_{0.63}$, respectively. $e^{(3)}_{100}$ shows the threefold degeneracies of e_{100}.

	This work		Experiment (Ref. 43)		Elsässer *et al.* (Ref. 6)	
$e^{(d)}_{nml}$	PdH	$PdH_{0.25}$	α or β		PdH	$PdH_{0.25}$
e_{000}	83.6	99.1				
$e^{(3)}_{100}$	59.3		β	60.0	62.0	
		71.0	α	69 ± 0.5		83.0
$e^{(3)}_{110}$	113.8	134.2	α	115 ± 5	117.0	158.0
$e^{(1)}_{200}$	126.5	147.3	α	137 ± 2	132.0	179.0
$e^{(2)}_{200}$	143.5	162.9	α	156 ± 3	147.0	197.0

to this case. Another reason is that Pd atoms make the potential steeper. Since the lattice vector in the a_z direction is much smaller than that in the a_x direction (for H in the O_1 site of $Pd_{0.25}Ag_{0.75}H_{0.25}$ and H in the O_2 site of $Pd_{0.5}Ag_{0.5}H_{0.25}$).

B. Absorption energies of H

The absorption energies of H in PdH_x and $Pd_{1-x}Ag_xH_{0.25}$ are calculated from the formula,

$$E_{\rm abs}=E_{rl}(Pd_{1-x}Ag_x)+\frac{1}{2}E_{(H_2)}-E_{rl}(Pd_{1-x}Ag_xH)$$
$$-E_{\rm zp1}(H)+E_{\rm zp2}(H) \quad (2)$$

where E_{rl} is the energy of the rigid lattice. $E_{(H_2)}$ is the total energy of the H_2 molecule ($E_{(H_2)}=-6.8037$ eV). $E_{\rm zp1}$ is the ZP energy of H in the octahedral site of the alloys. $E_{\rm zp2}$ is the ZP energy of H in the H_2 molecule ($E_{\rm zp2}=134.7$ meV per H atom). The calculated absorption energies per H atom in PdH_x and $Pd_{1-x}Ag_xH_{0.25}$ as a function of x are plotted in Figs. 4 and 5, respectively. For H in PdH_x, the calculated energy of 0.10 eV of H in $Pd_{32}H$ agrees very well with that of 0.10 eV of H in the heat solution in the experiment.[5] Figure 4 shows the energies increase with increasing H concentrations. The ZP energies of H decrease with increasing H concentrations (see Fig. 3), which partly contributes to the increasing energies. This tendency also means the H-H interaction is attractive in this case, which was also concluded by Christensen *et al.*[45] based on the effective-medium theory. However, the curve behavior in Fig. 4 is somewhat different from that of Christensen *et al.* The energies presented there increase continuously with increasing H concentrations. However, the results here show the maximum energy is found when x is 0.5. The present result seems to be more reasonable if we compare Fig. 4 with the phase diagram.[5,46] The reason for the maximum is unclear. This may be due to the electronic or geometric effect (or both). Further investigation is necessary.

Figure 5 shows the absorption energy per H atom in $Pd_{1-x}Ag_xH_{0.25}$ alloys as a function of x. It shows that the calculated curve behavior coincides well with that of the experiment.[47] When x is 0.25, the calculated energy of 0.32 eV of H in $Pd_{0.75}Ag_{0.25}H_{0.25}$ (H in the O_1 site) is larger than that of 0.17 eV of H in $PdH_{0.25}$. This indicates that H solubility in $Pd_{0.75}Ag_{0.25}H_{0.25}$ is significantly higher than that in $PdH_{0.25}$. This coincides with the experimental observation.[48] In Table II, we can see the lattice constant of 4.06 Å in $Pd_{0.75}Ag_{0.25}H_{0.25}$ is slightly larger than that of 4.02 Å in $PdH_{0.25}$. It seems that the increased lattice makes the octahedral site more favorable for H occupation. This seems to be a common rule if we compare the absorption energies of the comparable sites (see Table I for the comparable site). Take for an example, a comparison between $AgH_{0.25}$ and $Pd_{0.25}Ag_{0.75}H_{0.25}$ (H in the O_2 site). It shows that the lattice constant of $AgH_{0.25}$ is larger than that of $Pd_{0.25}Ag_{0.75}H_{0.25}$. Thus, the energy of H in $AgH_{0.25}$ is larger than that of H in

TABLE V. The calculated ZP and excitation energies of the vibrations of H in the O_1 and O_2 sites of $Pd_{4-x}Ag_x$ (in meV). The energies below are determined by the harmonic approximation. $e^{(2)}_{100}$ shows the twofold degeneracies of e_{100} and e_{010}. Some e_{002} is blank because the energies are too large.

	$Pd_{0.75}Ag_{0.25}H_{0.25}$		$Pd_{0.5}Ag_{0.5}H_{0.25}$		$Pd_{0.25}Ag_{0.75}H_{0.25}$		$AgH_{0.25}$
States	O_1	O_2	O_1	O_2	O_1	O_2	Octahedral site
			Anharmonic calculation				
e_{000}	95.8	101.6	97.9	110.1	114.9	92.9	91.8
$e^{(2)}_{100}$	68.8	64.8	60.8	47.5	57.7	65.5	65.1
e_{001}	68.8	88.5	90.4	137.3	123.9	65.5	65.1
e_{110}	130.2	121.0	113.0	88.2	109.5	123.0	123.0
$e^{(2)}_{101}$	130.2	146.3	144.8	177.1	174.8	123.0	123.0
e_{200}	142.8	141.2	133.8	106.2	133.5	133.9	134.0
e_{020}	158.0	155.6	148.9	119.2	124.9	150.3	148.7
e_{002}	158.0	185.9	—	—	—	150.3	148.7
			Harmonic approximation				
e_{000}	83.7	79.8	85.5	77.0	89.8	46.1	65.7
$e^{(2)}_{100}$	55.8	47.6	50.2	43.6	52.9	30.8	43.8
e_{001}	55.8	64.2	70.7	66.8	73.8	30.8	43.8

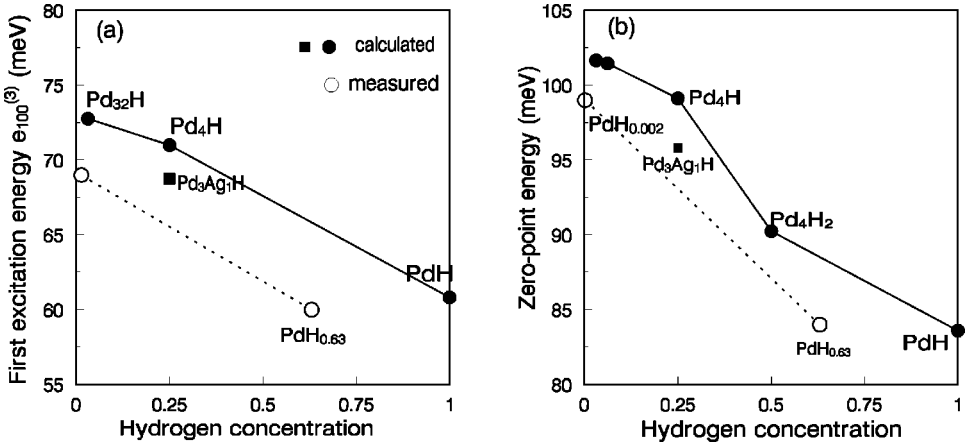

FIG. 3. The calculated (solid circles) and measured (open circles) ZP and excitation energies of H in PdH_x as a function of x. (a) and (b) are the first excitation energies and the ZP energies, respectively. The experimental data in (b) are from Ref. 44. The calculated energies of H in the O_1 site of $Pd_{0.75}Ag_{0.25}H_{0.25}$ are also given in the figure.

$Pd_{0.25}Ag_{0.75}H_{0.25}$. This rule was also observed theoretically by other authors[16] who concluded that the most stable sites have Ag as the next-nearest atoms. When x is larger than 0.5, Fig. 5 shows the energies decrease significantly with increasing Ag concentrations. This is in accordance with the experimental observation,[48] where the solubility of H in the Pd-Ag alloys decreases greatly when the Ag concentration is larger than 50%. For H in pure silver, The energy of -0.76 eV of H in $AgH_{0.25}$ indicates that this structure is extremely unstable. This is in accordance with the experimental observations,[49,50] where there is an extremely low hydrogen solubility in pure Ag.

The site occupation of H in the various interstitial sites of metals is an important topic.[21–24] For H in pure Pd, the absorption energy of H in the octahedral site is 81.4 meV more stable than that of H in the tetrahedral site. So the octahedral site is preferred by H. This is in accordance with the experiment.[21–24] For H in pure Ag ($AgH_{0.25}$), the absorption energy of -0.667 eV of H in the S_{110} site is in good agreement with the experimental value of -0.59 eV.[47] However, the occupation of H in the S_{110} expands the lattice constant greatly, which seems to be unphysical.[51] Considering the oscillation energies, we found that the energy of 96.5 meV of H in the tetrahedral site is in good agreement with the experimental predication of 93 meV.[52] As a result, there are some uncertainties for the occupation of H in pure Ag. For H occupations in the alloys, the calculated results show H in O_1 sites are more stable than H in the O_2 sites in each structure (H can not be localized in the tetrahedral sites of the alloys if the ZP energies are considered).

C. Diffusion barriers and paths of H

The diffusion barriers calculated with and without relaxation of the heavy atoms are determined by the saddle point search using the NEB method.[38] According to the absorption energies of H in the Pd-Ag alloys in Fig. 5, there is an extremely low H solubility in the Ag-rich areas exemplified by H in $Pd_{0.5}Ag_{0.5}H_{0.25}$, $Pd_{0.25}Ag_{0.75}H_{0.25}$ and $AgH_{0.25}$. This indicates that as it diffuses, H will avoid the Ag-rich areas. This coincides with the result of Opara *et al.*[49] who drew this conclusion based on an experiment and a simple model. Considering this, we would not discuss H diffusion in these structures. The rest of the paper mainly focuses on H diffu-

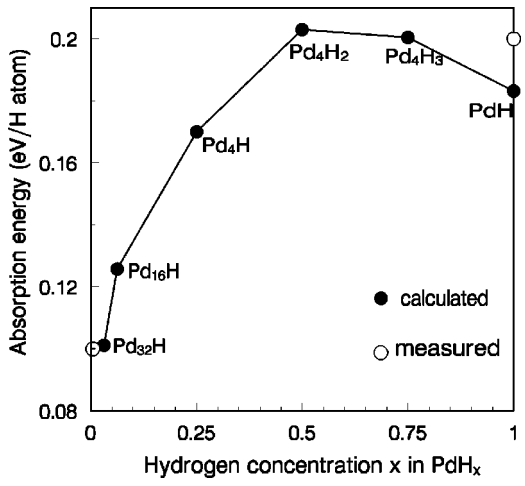

FIG. 4. The calculated and measured absorption energies of H in PdH_x as a function of x ($x=0.03125$, 0.0625, 0.25, 0.5, 0.75, and 1).

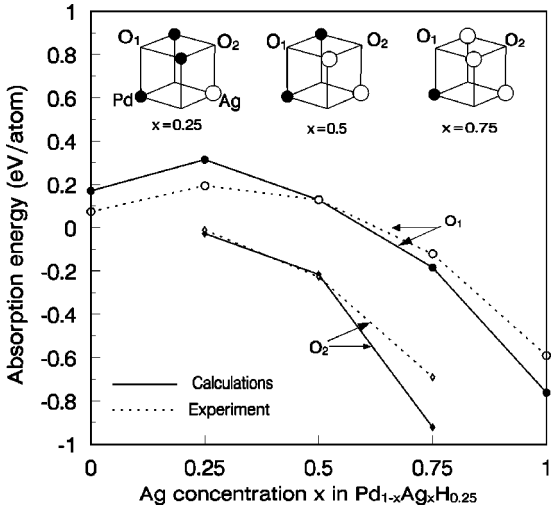

FIG. 5. Calculated (solid symbols) and measured (open symbols) absorption energies of H in $Pd_{1-x}Ag_xH_{0.25}$ as a function of x ($x=0$, 0.25, 0.5, 0.75, and 1). Experimental data are from the fittings of Ref. 47.

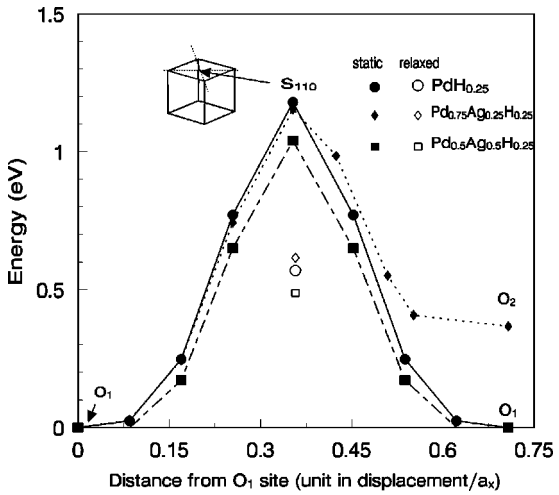

FIG. 6. Energy vs displacement curves with H diffusions along ''direct'' paths in $PdH_{0.25}$, $Pd_{0.75}Ag_{0.25}H_{0.25}$ and $Pd_{0.5}Ag_{0.5}H_{0.25}$. The total energy of H in the corresponding O_1 site is chosen as zero.

sion in $PdH_{0.25}$ and $Pd_{0.75}Ag_{0.25}H_{0.25}$. Next to that, H diffusion in $Pd_{0.5}Ag_{0.5}H_{0.25}$ between the O_1 sites is mentioned.

In the literature,[10,11,13,53,54] H diffusion in Pd is considered along two different paths. One is the so-called ''direct'' diffusion path, where H diffuses directly from one octahedral site to the next along the $\langle 110\rangle$ direction. The transition state for ''direct'' is denoted as S_{110} in Fig. 1(d). The other is the ''indirect'' path, where H diffusion is from an octahedral to tetrahedral site along the $\langle 111\rangle$ direction. From there H atom may move on to another octahedral site along one of the $\langle 111\rangle$ directions. Between the octahedral and tetrahedral site H passes the S_{111} transition state. The energy profiles for H diffusions along the ''direct'' and ''indirect'' paths are plotted in Figs. 6 and 7, respectively.

Figure 7 shows the energy profiles for H diffusions along ''indirect'' paths in $PdH_{0.25}$ and $Pd_{0.75}Ag_{0.25}H_{0.25}$. The inset pictures in Fig. 7 represent the preferred diffusion trajectories. For H diffusion in $PdH_{0.25}$, the diffusion barriers calculated with and without relaxation of the heavy atoms are 129 and 284 meV, respectively. For H diffusion in $Pd_{0.75}Ag_{0.25}H_{0.25}$, Fig. 7(b) shows there are two different transition states denoted as S^1_{110} and S^2_{110}. The barrier of 591 meV in S^2_{110} is significantly larger than that of 319 meV in S^1_{110}. This indicates that H diffusion to the Ag-rich area is hindered by a large barrier (O_2 site surrounded by two Ag and four Pd atoms). Fig. 7 (b) shows the local minimum between S^1_{110} and S^2_{110} is quite shallow compared to the relatively deep local minimum in $PdH_{0.25}$ (around the tetrahedral site). This indicates that H can not be localized in this minimum if the ZP energy is included. The inset picture in Fig. 7(b) shows that the trajectory of H diffusion in $Pd_{0.75}Ag_{0.25}H_{0.25}$ is almost along the $\langle 111\rangle$ direction before H reaches the local minimum, which is similar to that of $PdH_{0.25}$ in Fig. 7(a). After passing the local minimum, the trajectory has a large deviation from the $\langle 111\rangle$ direction. For H diffusion in $Pd_{0.5}Ag_{0.5}H_{0.25}$ between the O_1 sites, the diffusion path is similar to that of $PdH_{0.25}$ (not plotted).

TABLE VI. The ''direct'' (S_{110}) and ''indirect'' (S_{111}) diffusion barriers of H in $PdH_{0.25}$, $Pd_{0.75}Ag_{0.25}H$, and $Pd_{0.5}Ag_{0.5}H_{0.25}$ (in meV).

	Unrelaxed barrier		Relaxed barrier	
	S_{110}	S_{111}	S_{110}	S_{111}
$PdH_{0.25}$	1180	284	541	129
$Pd_{0.75}Ag_{0.25}H_{0.25}$	1155	591	594	315
$Pd_{0.5}Ag_{0.5}H_{0.25}$	1040	345	446	211

The diffusion barriers calculated with and without relaxation of the heavy atoms in Figs. 6 and 7 are summarized in Table VI. It shows that the corresponding barrier in the ''indirect'' path is much lower than that in the ''direct'' path, indicating that the preferred diffusion paths are ''indirect'' paths. The remainder of the diffusion barriers in this paper are given in terms of the ''indirect'' paths. For H diffusion in pure Pd, the measured barriers are between 230 and 300 meV.[22,55–58] If the ZP energies are included, the barriers calculated with and without the relaxation are 204.0 and 387.7 meV, respectively. Obviously, the barrier in the relaxed case is much closer to the observed barriers. It is noted that the

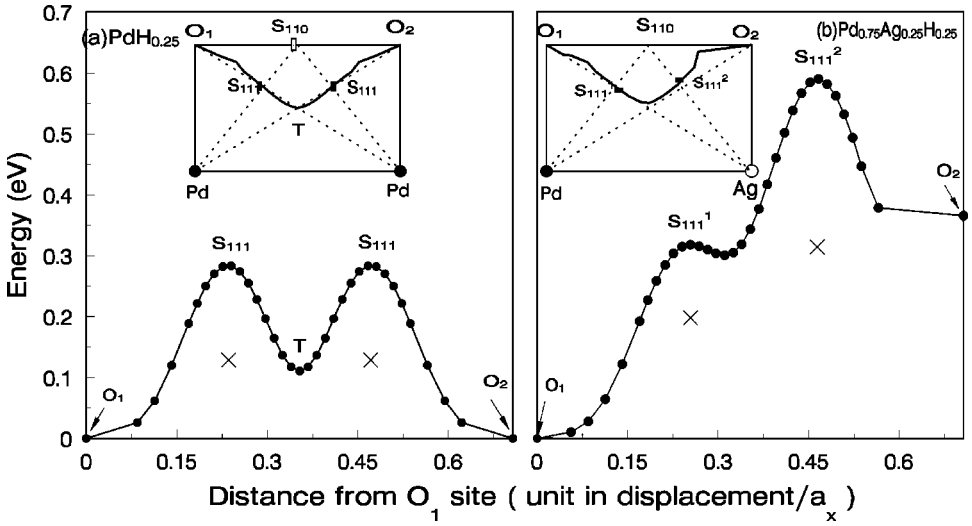

FIG. 7. Energy vs displacement curves with H diffusions along ''indirect'' paths in $PdH_{0.25}$ and $Pd_{0.75}Ag_{0.25}H_{0.25}$. The results are calculated with (solid line) and without (denoted as $\times$) relaxation of the heavy atoms. The inset pictures represent the preferred diffusion paths. The total energy of H in the O_1 site is chosen as zero.

TABLE VII. The energy levels (meV) and quantumn tunneling frequencies (s^{-1}) of H isotopes in $PdH_{0.25}$. The results are derived from the 1D PES (see the text for details).

	H		Deuterium		Tritium	
The states	Levels	Frequencies	Levels	Frequencies	Levels	Frequencies
ground state	16.2	5.59×10^{4}	9.2	1.97×10^{1}	6.2	0.0×10^{0}
first excitation	65.8	3.75×10^{6}	42.1	6.40×10^{3}	32.1	1.97×10^{1}
second excitation	124.3	3.66×10^{8}	81.1	1.34×10^{5}	62.6	5.92×10^{2}
third excitation	185.4	2.55×10^{10}	123.4	6.55×10^{6}	96.2	1.53×10^{4}
fourth excitation	243.7	3.91×10^{12}	166.9	3.62×10^{8}	131.3	1.30×10^{6}
fifth excitation			209.6	1.60×10^{10}	166.9	2.66×10^{7}
sixth excitation			249.4	1.72×10^{11}	202.0	9.14×10^{9}
seventh excitation					235.6	2.61×10^{10}
eighth excitation					266.1	4.40×10^{11}

barrier of 387.7 meV calculated without the relaxation does not differ very much from the measured values. This reflects the possibility that the heavy atom lattice has almost no time to respond in the case of a very quick jump. According to the above analysis, we conclude that the relaxation of the heavy atoms is important for the height of the diffusion barrier, and the real diffusion barrier should be somewhat larger than the barrier calculated with the relaxation.

The diffusion of H isotopes in bulk Pd shows an interesting isotope effect (IE): the diffusion constant of deuterium (D) is greater than that of H, which in turn is greater than that of tritium (T).[17] The IE between H and D (the heavier isotope diffuses more rapidly than the lighter one) shows the reversed IE effect. Despite many classical and quantum rate models for H diffusion in metals,[18–20,59] the understanding for the anomalous IE still is not fully clear. Obviously, the classical rate theory fails to explain the reversed IE, and it predicts that the sequence of the constants: $D_H > D_D > D_T$. Jost and Widman[18] explained the reversed IE successfully by using the quantum mechanical modified classical rate theory. Later, Sicking[20] pointed out this theory cannot explain why T diffusion is the slowest (it predicts T diffusion to be the fastest). As a solution, a ''quantum leak'' mechanism was proposed by Sicking[20] who assumed that H and D tunnel in their excited state E_n, and T tunnel in the higher energy state E_m $(m>n)$ [the potential there is very similar to Fig. 9(a)]. In this way he obtained the sequence of activation energies $E_T > E_D > E_H$ [see the arrows in Fig. 9(a)]. Although the assumption sounds reasonable, it was not underpinned by further theoretical evidence.

To verify Sicking's assumption,[20] we fit the 1D finite potential [Fig. 9(a)] to the 22nd order polynomial. The energy splittings are determined by solving the time-independent Schrödinger[36] based on the polynomial. The calculated quantum tunneling frequencies of H isotopes are compiled in Table VII according to expression

$$v_n = \frac{\Delta E}{h}, \tag{3}$$

where ΔE is the energy splitting and h is Plank's constant. Using these frequencies, we can evaluate the jump frequency from

$$v_t = \frac{\sum_{n=0}^{n_i} v_n \exp\left(\frac{-E_n}{kT}\right)}{\sum_{n=0}^{n_i} \exp\left(\frac{-E_n}{kT}\right)}, \tag{4}$$

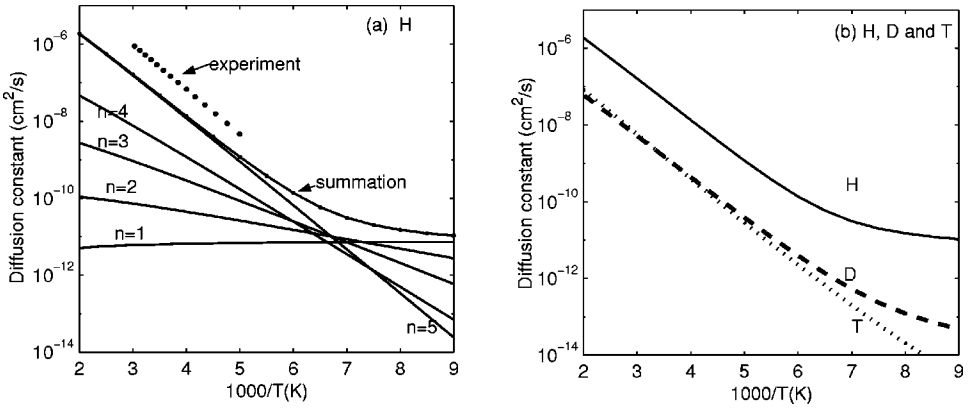

FIG. 8. The temperature dependence of the tunneling diffusion constants of H isotopes in $PdH_{0.25}$. In (a), the solid lines show the diffusion constants are contributed from the individual excitation states of H; the dotted solid line is the summation of the individual constant; the dotted points are for H diffusion in the α phase in the experiment (Ref. 17). (b) gives the comparisons of the diffusion constants of H isotopes (H in the solid line, D in the dashed line, and T in the dotted line).

TABLE VIII. The barrier energies (meV) and frequencies (s^{-1}) of the diffusions of H isotopes in $PdH_{0.25}$ for both unrelaxed and relaxed cases. The barriers include the ZP energies. The ZP energies in the octahedral site and in the saddle point were calculated by the 3D and 2D PES, respectively. v_o and v_s are frequencies for H isotopes in the octahedral site and in the saddle point, respectively.

	The unrelaxed case			The relaxed case	
	v_o	Barrier	v_s	Barrier	v_s
H	1.707×10^{13}	387.7	4.892×10^{13}	204.0	4.193×10^{13}
Deuterium	1.159×10^{13}	359.3	3.455×10^{13}	185.1	2.962×10^{13}
Tritium	9.271×10^{12}	346.2	2.824×10^{13}	175.1	2.418×10^{13}

where E_n corresponds to the n-th energy level of H isotopes, and k is the Boltzman constant. The diffusion constants are calculated without taking the effects of lattice deformations into account,

$$D_t=\frac{1}{6}L^2v_t, \tag{5}$$

where L is the distance between two nearest octahedral sites. The calculated tunneling diffusion constants of H isotopes are compiled in Fig. 8. At low temperatures, Fig. 8(a) shows that the constants are mainly dominated by the ground state tunneling effect. The occupation of the higher excited states is reduced at the low temperatures. With increasing temperatures, the higher excited states become thermally occupied, and thus the contributions from the higher excited states dominates the constants. Comparing the calculated constants of H with that of the experiment,[17] we find that the current results underestimate the experiment data. Fig. 8(b) compares the calculated diffusion constants of H isotopes. It shows that the constant of H is greater than that of D, which in turn is slightly greater than that of T. This indicates that the quantum tunneling effect of H is more than that of D, which is slightly more than that of T. The calculated results fail to explain the reversed IE.

If we calculate the constants according to the traditional 1D quantum transition-state rate theory,[60] the results seem to be much better. The expression is[60]

$$k=\frac{\omega_0}{2\pi}\exp(-\beta E^+)\frac{(\beta\hbar\omega^+/2)\sinh(\beta\omega^+/2)}{(\beta\hbar\omega_0/2)\sinh(\beta h\omega_0/2)}, \tag{6}$$

where E^+ is the activation energy, ω_0 and ω^+ are the vibrational frequencies in the octahedral site and in the saddle point, respectively. The barriers including the ZP energies and frequencies are compiled in Table VIII and Fig. 9(c). Figure 10 shows that the calculated and measured temperature dependence of the diffusion constants of H isotopes in $PdH_{0.25}$. It shows the calculated diffusion constant for D is in quite good agreement with the experiment.[61] The calculated results for H underestimate the experimental data.[61] This implies that the quantum tunneling effect may make an important contribution to the constant. The calculated results can easily explain that the reversed IE ($D_D>D_H$). In Figs. 9(a) and 9(b), they show that T can easily be localized in the tetrahedral site of $PdH_{0.25}$. This indicates that the diffusion mechanism of T is different from that of H or D. For H or D, it just needs a jump from an octahedral site to another, but for T, it needs double jumps, where T first jumps from an octahedral site to the nearest tetrahedral site. From there it may jump back or jump forth, or just stay there due to the

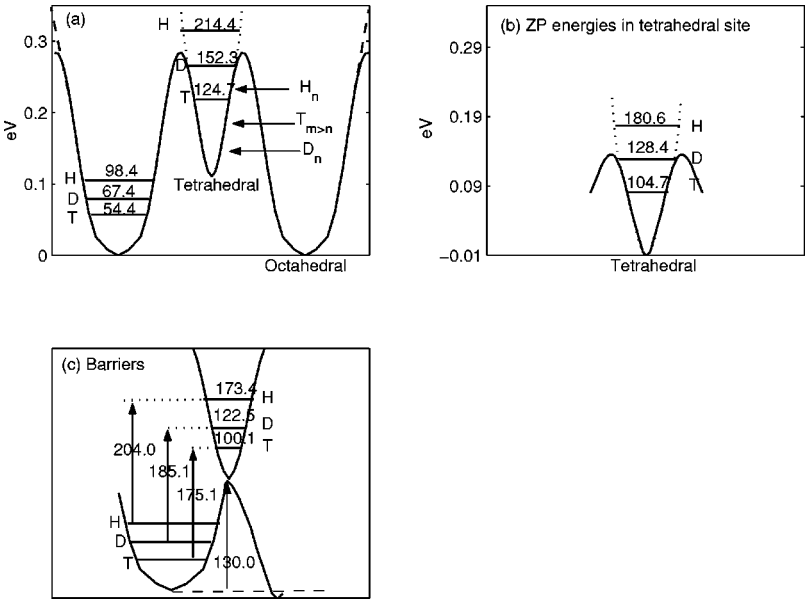

FIG. 9. The ZP energies of H isotopes in the octahedral (a) and tetrahedral (b) sites of $PdH_{0.25}$. The sequence of the energies of H_n, D_n and $T_{m>n}$ is ''quantum leak'' assumption proposed by Sicking (see the text for details). (c) gives the diffusion barriers of H isotopes in the relaxed lattice (including ZP energies). The ZP energies at the saddle point are determined by the 2D potential. Units are in meV's.

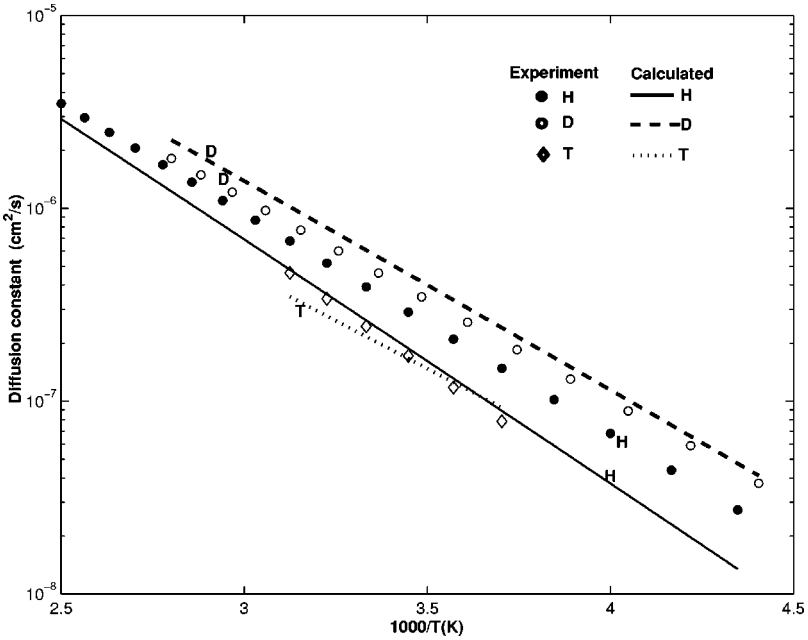

FIG. 10. The calculated and measured temperature dependence of the diffusion constants of H isotopes in $PdH_{0.25}$. The calculated results are determined from the 1D quantum transition-state theory. The experimental data are from the literature (Refs. 17 and 61).

possibility of the increases of barriers on both sides. The real diffusion process may be complicated. If we simply consider that T jumps $L/2$ distance for one jump in Eq. (5), surprisingly, the calculated constant agrees reasonably with the experimental data.[61] To some extent, this supports our proposed mechanism. In this way, the anomalous IE becomes quite clear now.

IV. CONCLUSIONS

The vibrational states, absorption energies, and diffusions of H in PdH_x ($x=0.03125$, 0.0625, 0.25, 0.5, 0.75, and 1) and $Pd_{1-x}Ag_xH_{0.25}$ ($x=0$, 0.25, 0.5, 0.75, and 1) have been studied by DFT.

The vibrational energies of H are determined by solving the time-independent Schrödinger equations based on the PESes. The results show that the harmonic approximation is inadequate to study the vibrations of H in Pd_xH and $Pd_{1-x}Ag_xH_{0.25}$. The lattice constant dependence of the vibrational energy is revealed. For the lower H concentrations in Pd (PdH_x, $x=0.031254$ and 0.25), our method seems to be somewhat of an improvement compared to that of Elsässer. The present results demonstrate that the total energy calculations are good enough to predict the vibrational energies even for the lower H concentrations. For H in some of the Pd-Ag alloys, the vibrational energy of e_{001} is significantly larger than that of e_{100}. Both Ag and Pd atoms may contribute to the steep vibrational potential for different reasons.

The calculated absorption energies of H in PdH_x and $Pd_{1-x}Ag_xH_{0.25}$ agree well with the experimental data. The calculated energy of H in the O_1 sites of the alloys (with Ag as the next-nearest neighbor) is much greater than that of H in the O_2 sites in each structure. The calculated energy of H in the O_1 site of $Pd_{0.75}Ag_{0.25}H_{0.25}$ is greater than that of H in $PdH_{0.25}$. The energies decrease significantly when $x \geqslant 0.5$. This indicates that the solubility of H in the Pd-Ag alloys increases when x is about 0.25, and decreases greatly when x is larger than 0.5. This coincides with the experimental observations. This also indicates that H diffusion to the Ag-rich region is strongly blocked.

The calculated diffusion path of H in $PdH_{0.25}$ is almost along the $\langle 111 \rangle$ direction. The diffusion path of H in $Pd_{0.75}Ag_{0.25}H_{0.25}$ has a large deviation from the $\langle 111 \rangle$ direction. According to the absorption energies and diffusion barriers, H diffusion in the Pd-Ag alloys should avoid the Ag-rich areas.

The interesting anomalous isotope effect is explored. The ZP energy of H in the saddle point is significantly greater than that of D. Thus the activation energy of H is greater than that of D. This is the main reason for the reversed IE. A diffusion process is proposed for tritium.

Due to the light mass of H, the ZP motion is very important in the determination of the absorption site and the diffusion barrier of H. In general, the ZP energies of H in the octaheral sites of pure Pd and Pd-Ag alloys are smaller than 120 meV, and the ZP energies of H in the tetrahedral sites are larger than 150 meV (see Tables IV and Table V). This means that the ZP energy of H in the octaheral site increases the absorption energy, and the ZP energy of H in the tetrahedral site decreases the absorption energy. For H absorption in $PdH_{0.25}$, the theoretical results show H in the tetrahedral site is 10.8 meV more stable than H in the octahedral site without considering the ZP motions. If the ZP energies are included, H in the octahedral site is 81.4 meV more stable than H in the tetrahedral site, and H cannot even be localized in the tetrahedral site (see Fig. 9). For H in the alloys, H cannot be localized in the tetrahedral sites either if the ZP motions are considered. The ZP motion plays a key role in explaining the reversed IE.

ACKNOWLEDGMENTS

The authors thank Dr. Tonek Jansen and Dr. Geert Jan Kroes for the useful discussions, and Dr. S. R. G. Ralston for

carefully reading the manuscript. X. K. would like to thank the friendly help from P. van Beurden, I. Ciobica, F. Frechard, V. Mihaleva, P. Vassilev, X. Rozanska, and S.J. Mitchell. This research was carried out under a grant from NWO (Netherlands Organization for Scientific Research) with financial contributions of Shell Global Solutions International, Senter and the Dutch Ministry of Environmental Affairs. NCF granted computer time on its TERAS supercomputer.

*Email address: ke@sg10.chem.tue.nl

[1] *The Palladium Hydrogen System*, edited by F. A. Lewis (Academic Press, London, 1967) pp. 48 and 94.

[2] *H in Metals I*, edited by G. Alefeld, and J. Völkl, Topics in Applied Physics Vol. 28 (Springer, Berlin, 1978); *ibid.*, Vol. 29.

[3] *H in Intermetallic Compounds I*, edited by Franz L. Schlapbach, Topics in Applied Physics Vol. 63 (Springer, Berlin, 1988).

[4] *Sputtering by Particle Bombardment III*, edited by R. Behrisch, and K. Wittmaack, Topics in Applied Physics Vol. 64 (Springer, Berlin, 1988).

[5] E. Wicke, H. Brodowsky, and H. Züchner, in *H in Metals I* (Ref. 2) p. 73.

[6] C. Elsässer, K.M. Ho, C.T. Chan, and M. Fähnle, Phys. Rev. B **44**, 10377 (1991).

[7] Lawrence R. Pratt and J. Eckert, Phys. Rev. **39**, 13170 (1989).

[8] B. M. Klein and R.E. Cohen, Phys. Rev. B **45**, 12405 (1992).

[9] Yan Wang, Sheng N. Sun, and M.Y. Chou, Phys. Rev. B **53**, 1 (1996).

[10] Y. Li and Göran Wahnström, Phys. Rev. B **46**, 14528 (1992).

[11] R. Löber and D. Hennig, Phys. Rev. B **55**, 4761 (1997).

[12] A. Gross and M. Scheffler, Phys. Rev. B **57**, 2493 (1998).

[13] R.A. Olsen, P.H.T. Philipsen, E.J. Baerends, G.J. Kroes, and O. M. Løvvik, J. Chem. Phys. **106**, 9286 (1997).

[14] Z. Sun and D. Tománek, Phys. Rev. Lett. **63**, 59 (1989).

[15] W. Dong and J. Hafner, Phys. Rev. B **56**, 15396 (1997).

[16] O.M. Løvvik, and R.A. Olsen, J. Alloys Compd. **330-332**, 332 (2002).

[17] J. Völkl and G. Alefeld, in *H in Metals I* (Ref. 2), Vol. 28, p. 321, and references cited therein.

[18] K. W. Kehr, in *H in Metals I* (Ref. 2), Vol. 28, p. 197 and references cited therein (p. 221).

[19] S.W. Rick, D.L. Lynch, and J.D. Doll, J. Chem. Phys. **99**, 8183 (1993).

[20] G. Sicking, Ber. Bunsenges. Phys. Chem. **76**, 790 (1972).

[21] J.M. Rowe, J.J. Rush, L.A. de Graaf, G.A. Ferguson, Phys. Rev. Lett. **29**, 1250 (1972).

[22] G. Nelin and K. Sköld, J. Phys. Chem. Solids **36**, 1175 (1975); K. Sköld and G. Nelin, *ibid.* **28**, 2369 (1967).

[23] J.E. Worsham, Jr., M.K. Wilkinson, and C.G. Shull, J. Phys. Chem. Solids **3**, 303 (1957).

[24] H.D. Carstanjen, Z. Phys. Chem. (Munich) **165**, 141 (1989).

[25] B.H. Brandsen and C.J. Joachain, *Physics of Atoms and Molecules* (Longman Scientific and Technical, Essex, England, 1991).

[26] *The Palladium Hydrogen System* (Ref. 1) p. 71; I. Karakaya and W.T. Thompson, in *Binary Alloy Phase Diagrams*, edited by T. B. Massalski (American Society of Metals, Metals Park, OH, 1986).

[27] G. Kresse and J. Furthmüller, Comput. Mater. Sci. **6**, 15 (1996).

[28] G. Kresse and J. Furthmüller, Phys. Rev. B **54**, 11169 (1996).

[29] J.P. Perdew, in *Electronic Structure of Solids '91*, edited by P. Ziesche, and H. Eschrig (Akademie Verlag, Berlin, 1991).

[30] D. Vanderbilt, Phys. Rev. B **41**, 7892 (1990).

[31] H.J. Monkhorst and J.D. Pack, Phys. Rev. B **13**, 5188 (1976).

[32] P.E. Blöchl, Phys. Rev. B **50**, 17953 (1994).

[33] G. Kresse and D. Joubert, Phys. Rev. B **59**, 1758 (1999).

[34] H. Rose, J. Ferrante, and J.R. Smith, Phys. Rev. Lett. **47**, 675 (1981).

[35] B.R. Coles, J. Inst. Met. **84**, 346 (1956).

[36] E.L. Meijer, R.A. van Santen, and A.P.J. Jansen, J. Phys. Chem. **100**, 9282 (1996).

[37] R. Löber and D. Hennig, Phys. Rev. B **55**, 4761 (1997).

[38] H. Jónsson, G. Mills, and K.M. Jacobsen, in *Nudged Elastic Band Method for Finding Minimum Energy Paths of Transitions in Classical and Quantum Dynamics in Condensed Phase Simulations*, edited by B.J. Berne, G. Ciccotti, and D.F. Coker (World Scientific, Singapore, 1998).

[39] The increasing H concentration in pure Pd or the increasing Ag concentration in Pd-Ag alloys leads to the increase of the lattice constant, resulting in the shallower vibrational PES, and thus to a lowering of the excitation energy (Ref. 7).

[40] J.M. Rowe, J.J. Rush, H.G. Smith, M. Mostoller, and H.E. Flotow, Phys. Rev. Lett. **33**, 1297 (1974).

[41] A. Rahman, K. Sköld, C. Pelizzari, S.K. Sinha, and H.E. Flotow, Phys. Rev. B **14**, 3630 (1976).

[42] C.J. Glinka, J.M. Rowe, J.J. Rush, A. Rahman, S.K. Sinha, and H.E. Flotow, Phys. Rev. B **17**, 488 (1978).

[43] J.J. Rush, J.M. Rowe, and D. Richter, Z. Phys. B: Condens. Matter **55**, 283 (1984).

[44] T. Springei, in *H in Metals I* (Ref. 2), Vol. 28 p. 75. The experimental data there are the optic frequncies of hydrogen. The ZP energies are estimated as three halves of these values.

[45] O.B. Christensen, P.D. Ditlevsen, K.W. Jacobsen, P. Stoltze, O.H. Nielsen, and J.K. Nørskov, Phys. Rev. B **40**, 1993 (1989).

[46] H.C. Jamieson, G.C. Weatherly, and F.D. Manchester, J. Less-Common Met. **50**, 85 (1976).

[47] H. Hemmes, E. Salomons, R. Griessen, P. Sänger, and A. Driessen, Phys. Rev. B **39**, 10606 (1989).

[48] The Palladium Hydrogen System (Ref. 1) p. 70. The maximum solubility of H in the Pd-Ag alloys is found there when Ag concentration is close to 20% or 30%, which depends on the temperatures.

[49] L. Opara, B. Klein, and H. Züchner, J. Alloys Compd. **253-254**, 378 (1997).

[50] P.R. Subramanian, in *Binary Alloy Phase Diagrams*, (Ref. 30) p. 42.

[51] Private communication with Dr. L.C. Witjens. Their (L.C. Witjens, A.J. van Dillen, J.H. Bitter, and K.P. de Jong) experiment (XAFS) showed that the lattice constant changes very little (about 0.01 Å) after exposure to H_2.

[52] A.I. Kolesnikov, V.E. Antonov, S. Bennington, M. Prager, and J. Tomkinson, Physica B **213-214**, 442 (1995).

[53] C. Elsässer, M. Fähnle, K.M. Ho, and C.T. Chan, Physica B **172**, 217 (1991).

[54] O.B. Christensen, P. Stoltze, K.W. Jacobsen, and J.K. Nørskov, Phys. Rev. B **41**, 12413 (1990).

[55] H. Kronmüller, G. Higelin, P. Vargas, and R. Lässer, Z. Phys. Chem., Neue Folge **143**, 161 (1985).
[56] E. Salomons, J. Phys.: Condens. Matter **2**, 845 (1990).
[57] A.H. Verbruggen, C.W. Hagen, and R. Griessen, J. Phys. F: Met. Phys. **14**, 1431 (1984).
[58] S. Majorewski and B. Baranowski, J. Phys. Chem. Solids **43**, 1119 (1982).
[59] H.R. Schober and A.M. Stoneham, Phys. Rev. Lett. **60**, 2307 (1988).
[60] P.G. Wolynes, Phys. Rev. Lett. **47**, 968 (1981).
[61] J. Völkl, G. Wollenweber, K.-H. Klatt, and G. Alefeld, Z. Naturforsch. **26A**, 922 (1971).